

International Journal of Modern Physics E
© World Scientific Publishing Company

CONSTRAINING THE SYMMETRY ENERGY: A JOURNEY IN THE ISOSPIN PHYSICS FROM COULOMB BARRIER TO DECONFINEMENT

M. DI TORO *, M. COLONNA, V. GRECO, G. FERINI, C. RIZZO, J. RIZZO

*Laboratori Nazionali del Sud INFN, I-95123 Catania, Italy,
and Physics-Astronomy Dept., University of Catania*

* E-mail: ditorio@lns.infn.it

V. BARAN

Dept. of Theoretical Physics, Bucharest Univ., and NIPNE-HH, Magurele, Bucharest, Romania

T. GAITANOS

Inst. für Theoretische Physik, Universität Giessen, D-35312 Giessen, Germany

V. PRASSA

Dept. of Theoretical Physics, Aristotle Univ. of Thessaloniki, Gr-54124, Greece

H. H. WOLTER

Dept. für Physik, Universität München, D-85748 Garching, Germany

M. ZIELINSKA-PFABE

Smith College, Northampton, Mass. USA

Received October 07

Revised October 07

Heavy Ion Collisions (*HIC*) represent a unique tool to probe the in-medium nuclear interaction in regions away from saturation. In this work we present a selection of reaction observables in dissipative collisions particularly sensitive to the isovector part of the interaction, i.e. to the symmetry term of the nuclear Equation of State (*EOS*). At low energies the behavior of the symmetry energy around saturation influences dissipation and fragment production mechanisms. We will first discuss the recently observed Dynamical Dipole Radiation, due to a collective neutron-proton oscillation during the charge equilibration in fusion and deep-inelastic collisions. Important *Iso* – *EOS* are stressed. Reactions induced by unstable ^{132}Sn beams appear to be very promising tools to test the sub-saturation Isovector *EOS*. New Isospin sensitive observables are also presented for deep-inelastic, fragmentation collisions and Isospin equilibration measurements (Imbalance Ratios).

The high density symmetry term can be derived from isospin effects on heavy ion reactions at relativistic energies (few *AGeV* range), that can even allow a “direct” study of the covariant structure of the isovector interaction in the hadron medium. Rather sensitive observables are proposed from collective flows and from pion/kaon produc-

tion. The possibility of the transition to a mixed hadron-quark phase, at high baryon and isospin density, is finally suggested. Some signatures could come from an expected “neutron trapping” effect. The importance of studying violent collisions with radioactive beams from low to relativistic energies is finally stressed.

Keywords: Charge Equilibration, Symmetry Energy, Isospin Transport, Isospin Flows, Particle Production, Deconfinement

1. Introduction

The symmetry energy E_{sym} appears in the energy density $\epsilon(\rho, \rho_3) \equiv \epsilon(\rho) + \rho E_{sym}(\rho_3/\rho)^2 + O(\rho_3/\rho)^4 + \dots$, expressed in terms of total ($\rho = \rho_p + \rho_n$) and isospin ($\rho_3 = \rho_p - \rho_n$) densities. The symmetry term gets a kinetic contribution directly from basic Pauli correlations and a potential part from the highly controversial isospin dependence of the effective interactions¹. Both at sub-saturation and supra-saturation densities, predictions based of the existing many-body techniques diverge rather widely, see². We remind that the knowledge of the *EoS* of asymmetric matter is very important at low densities (neutron skins, nuclear structure at the drip lines, neutron distillation in fragmentation, neutron star formation and crust..) as well as at high densities (transition to a deconfined phase, neutron star mass/radius, cooling, hybrid structure, formation of black holes...). We take advantage of new opportunities in theory (development of rather reliable microscopic transport codes for *HIC*) and in experiments (availability of very asymmetric radioactive beams, improved possibility of measuring event-by-event correlations) to present results that are severely constraining the existing effective interaction models. We will discuss dissipative collisions in a wide range of energies, from just above the Coulomb barrier up to a few *AGeV*. Low to Fermi energies will bring information on the symmetry term around (below) normal density, relativistic energies will probe high density regions, even testing the covariant structure of the isovector terms. The transport codes are based on mean field theories, with correlations included via hard nucleon-nucleon elastic and inelastic collisions and via stochastic forces, selfconsistently evaluated from the mean phase-space trajectory, see^{1,3,4,5}. Stochasticity is essential in order to get distributions as well as to allow the growth of dynamical instabilities. The isovector part of the *EoS* has been tested systematically by using two different behaviors of the symmetry energy below saturation: one (*Asysoft*) where it is a smooth decreasing function towards low densities, and another one (*Asystiff*) where we have a rapid decrease,^{1,6}.

2. The Prompt Dipole γ -Ray Emission

The possibility of an entrance channel bremsstrahlung dipole radiation due to an initial different N/Z distribution was suggested at the beginning of the nineties^{7,8}. After several experimental evidences, in fusion as well as in deep-inelastic reactions^{9,10,11,12,13,14} we have now a good understanding of the process and stimulating new perspectives from the use of radioactive beams.

During the charge equilibration process taking place in the first stages of dissipative reactions between colliding ions with different N/Z ratios, a large amplitude dipole collective motion develops in the composite dinuclear system, the so-called dynamical dipole mode. This collective dipole gives rise to a prompt γ -ray emission which depends: i) on the absolute value of the initial dipole moment

$$D(t=0) = \frac{NZ}{A} |R_Z(t=0) - R_N(t=0)| = \frac{R_P + R_T}{A} Z_P Z_T \left| \left(\frac{N}{Z}\right)_T - \left(\frac{N}{Z}\right)_P \right|, \quad (1)$$

being $R_Z = \frac{\sum_i x_i(p)}{Z}$ and $R_N = \frac{\sum_i x_i(n)}{N}$ the center of mass of protons and of neutrons respectively, while R_P and R_T are the projectile and target radii; ii) on the fusion/deep-inelastic dynamics; iii) on the symmetry term, below saturation, that is acting as a restoring force.

A detailed description is obtained in a microscopic approach based on semi-classical transport equations, of Landau-Vlasov type,¹⁵ where mean field and two-body collisions are treated in a self-consistent way, see details in^{16,17}. Realistic effective interactions of Skyrme type are used. The resulting physical picture is in good agreement with quantum Time-Dependent-Hartree-Fock calculation¹⁸. In particular we can study in detail how a collective dipole oscillation develops in the entrance channel¹⁷.

We can follow the time evolution of the dipole moment in the r -space, $D(t) = \frac{NZ}{A}(R_Z - R_N)$ and in p -space, $DK(t) = (\frac{P_p}{Z} - \frac{P_n}{N})$, with P_p (P_n) center of mass in momentum space for protons (neutrons), is just the canonically conjugate momentum of the $D(t)$ coordinate, i.e. as operators $[D(t), DK(t)] = i\hbar$ see^{17,18,19}. A nice "spiral-correlation" clearly denotes the collective nature of the mode.

From the dipole evolution given from the Landau-Vlasov transport we can directly apply a bremsstrahlung ("bremss") approach¹⁹ to estimate the "direct" photon emission probability ($E_\gamma = \hbar\omega$):

$$\frac{dP}{dE_\gamma} = \frac{2e^2}{3\pi\hbar c^3 E_\gamma} |D''(\omega)|^2, \quad (2)$$

where $D''(\omega)$ is the Fourier transform of the dipole acceleration $D''(t)$. We remark that in this way it is possible to evaluate, in *absolute* values, the corresponding pre-equilibrium photon emission.

We must add a couple of comments of interest for the experimental selection of the Dynamical Dipole: i) The centroid is always shifted to lower energies (large deformation of the dinucleus); ii) A clear angular anisotropy should be present since the prompt mode has a definite axis of oscillation (on the reaction plane) at variance with the statistical *GDR*. In a very recent experiment the prompt dipole radiation has been investigated with a 4π gamma detector. A strong dipole-like photon angular distribution (θ_γ) = $W_0[1 + a_2 P_2(\cos\theta_\gamma)]$, θ_γ being the angle between the emitted photon and the beam axis, has been observed, with the a_2 parameter close to -1 , see¹⁴.

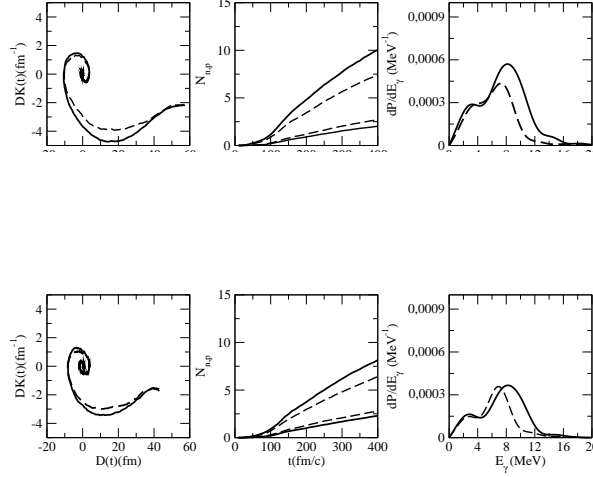


Fig. 1. Upper Curves: $^{132}\text{Sn} + ^{58}\text{Ni}$ system ($E = 10\text{MeV}$, $b = 4\text{fm}$). Lower Curves: same reactions but induced by ^{124}Sn . Left Panel: DK-D Spirals. Central panel: neutron (upper) and proton (lower) emissions. Right panel: γ spectrum. Asy-soft (solid lines) and asy-stiff (dashed lines) symmetry energies.

The deviation from a *pure* dipole form can be interpreted as due to the rotation of the dinucleus symmetry axis vs. the beam axis during the Prompt Dipole Emission. From accurate angular distribution measurements we can then expect to get a direct information on the Dynamical Dipole Life Time.

At higher beam energies we expect a decrease of the direct dipole radiation for two main reasons both due to the increasing importance of hard NN collisions: i) a larger fast nucleon emission that will equilibrate the isospin before the collective dipole starts up; ii) a larger damping of the collective mode due to np collisions.

The prompt dipole radiation also represents a nice cooling mechanism on the fusion path. It could be a way to pass from a *warm* to a *cold* fusion in the synthesis of heavy elements with a noticeable increase of the *survival* probability,²⁰

$$\frac{P_{surv,dipole}}{P_{surv}} = \frac{P_{\gamma}P_{surv}(E^* - E_{\gamma})}{P_{surv}(E^*)} + (1 - P_{\gamma}) > 1, \quad \frac{P_{surv}(E^* - E_{\gamma})}{P_{surv}(E^*)} > 1 \quad (3)$$

Symmetry Energy Effects

The use of unstable neutron rich projectiles would largely increase the effect, due to the possibility of larger entrance channel asymmetries. In order to suggest proposals for the new *RIB* facility *Spiral 2*,²¹ we have studied fusion events in the reaction $^{132}\text{Sn} + ^{58}\text{Ni}$ at 10MeV ,²². We expect a *Monster* Dynamical Dipole, the initial dipole moment $D(t = 0)$ being of the order of 50fm , about two times the largest values probed so far, allowing a detailed study of the symmetry potential, below saturation, responsible of the restoring force of the dipole oscillation and even of the damping, via the fast neutron emission. In the Fig.1 (upper) we present some

preliminary very promising results. The larger value of the symmetry energy for the *Asysoft* choice at low densities, where the prompt dipole oscillation takes place, leads to some clear observable effects: i) Larger Yields, as we see from the larger amplitude of the "Spiral" (left panel) and finally in the spectra (right panel); ii) Larger mean gamma energies, shift of the centroid to higher values in the spectral distribution (right panel); iii) Larger width of the "resonance" (right panel) due to the larger fast neutron emission (central panel). We note the opposite effect of the Asy-stiffness on neutron vs proton emissions. The latter point is important even for the possibility of an independent test just measuring the N/Z of the pre-equilibrium nucleon emission.

The symmetry energy influence can be of the order of 20%, and so well detected. In the lower part of the same figure we present the same results for reactions induced by the stable ^{124}Sn beam. We still see the *Iso* – *EoS* effects, but largely reduced.

3. Isospin Dynamics in Neck Fragmentation at Fermi Energies

It is now quite well established that the largest part of the reaction cross section for dissipative collisions at Fermi energies goes through the *Neck Fragmentation* channel, with *IMFs* directly produced in the interacting zone in semiperipheral collisions on very short time scales^{23,24}. We can predict interesting isospin transport effects for this new fragmentation mechanism since clusters are formed still in a dilute asymmetric matter but always in contact with the regions of the projectile-like and target-like remnants almost at normal densities. Since the difference between local neutron-proton chemical potentials is given by $\mu_n - \mu_p = 4E_{\text{sym}}(\rho_3/\rho)$, we expect a larger neutron flow to the neck clusters for a stiffer symmetry energy around saturation,^{1,25}. The isospin dynamics can be directly extracted from correlations between N/Z , *alignment* and emission times of the *IMFs*. The alignment between *PLF* – *IMF* and *PLF* – *TLF* directions represents a very convincing evidence of the dynamical origin of the mid-rapidity fragments produced on short time scales²⁶. The form of the Φ_{plane} distributions (centroid and width) can give a direct information on the fragmentation mechanism²⁷. Recent calculations confirm that the light fragments are emitted first, a general feature expected for that rupture mechanism²⁸. The same conclusion can be derived from *direct* emission time measurements based on deviations from Viola systematics observed in event-by-event velocity correlations between *IMFs* and the *PLF/TLF* residues^{26,27,29}. We can figure out a continuous transition from fast produced fragments via neck instabilities to clusters formed in a dynamical fission of the projectile(target) residues up to the evaporated ones (statistical fission). Along this line it would be even possible to disentangle the effects of volume and shape instabilities. A neutron enrichment of the overlap ("neck") region is expected, due to the neutron migration from higher (spectator) to lower (neck) density regions, directly related to the slope of the symmetry energy²⁸. A very nice new analysis has been presented on the $\text{Sn} + \text{Ni}$ data at 35 AMeV by the Chimera Collab., Fig.2 of ref.³⁰. A strong correlation between

neutron enrichment and alignment (when the short emission time selection is enforced) is seen, that can be reproduced only with a stiff behavior of the symmetry energy. *This is the first clear evidence in favor of a relatively large slope (symmetry pressure) around saturation.*

4. Isospin Distillation with Radial Flow

In central collisions at 30-50 MeV/A, where the full disassembly of the system into many fragments is observed, one can study specifically properties of liquid-gas phase transitions occurring in asymmetric matter^{31,32,5,1}. For instance, in neutron-rich matter, phase co-existence leads to a different asymmetry in the liquid and gaseous phase: fragments (liquid) appear more symmetric with respect to the initial matter, while light particles (gas) are more neutron-rich. The amplitude of this effect depends on specific properties of the isovector part of the nuclear interaction, namely on the value and the derivative of the symmetry energy at low density.

This investigation is interesting in a more general context: In heavy ion collisions the dilute phase appears during the expansion of the interacting matter. Thus we study effects of the coupling of expansion, fragmentation and distillation in a two-component (neutron-proton) system. We present fully consistent dynamical results, based on stochastic microscopic transport approaches widely tested in heavy ion collisions^{5,1,3,4,33}. The correct treatment of fluctuations is essential to reproduce the dynamics of spinodal instabilities in the dilute expansion phase.

We focus on central collisions, $b = 2 fm$, considering symmetric reactions between systems having three different initial asymmetry: $^{112}Sn + ^{112}Sn$, $^{124}Sn + ^{124}Sn$, $^{132}Sn + ^{132}Sn$, with $(N/Z)_{in} = 1.24, 1.48, 1.64$, respectively. The considered beam energy is 50 MeV/A. 1200 events have been run for each reaction and for each of the two symmetry energies adopted (asy-soft and asystiff, see before)³⁴.

In central collisions, after the initial collisional shock, the system expands and breaks up into many pieces, due to the development of volume (spinodal) and surface instabilities. The formation of a bubble-like configuration is observed, where the initial fragments are located.

First, let us briefly recall some general features concerning the isotopic content of fragments and emitted nucleons, as obtained with the two considered iso-EOS's. In the following we will restrict our analysis to fragments with charge in the range between 3 and 10 (that we call intermediate mass fragments (IMF's)). The average N/Z of emitted nucleons (gas phase) and IMF's is presented in Fig.2 as a function of the initial $(N/Z)_{in}$ of the three colliding systems. One observes that, generally, the gas phase (right panel) is more neutron-rich in the asysoft case, while IMF's (left panel) are more symmetric. This is due to the larger value of the symmetry energy at low density for the asysoft parameterization³³. It is interesting to note that, in the asystiff case, due to the rather low value of the symmetry energy, Coulomb effects dominate and the N/Z of the gas phase becomes lower than that for IMF's,

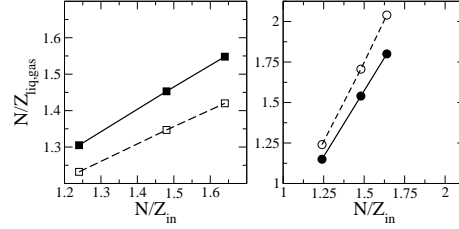


Fig. 2. The N/Z of the liquid (left) and of the gas (right) phase is displayed as a function of the system initial N/Z . Full lines and symbols refer to the asystiff parameterization. Dashed lines and open symbols are for asysoft.

because protons are preferentially emitted. Now we move to investigate in more detail correlations between fragment isotopic content and kinematical properties. The idea in this investigation is that fragmentation originates from the break-up of a composite source that expands with a given velocity field. Since neutrons and protons experience different forces, one may expect a different radial flow for the two species. In this case, the N/Z composition of the source would not be uniform, but would depend on the radial distance from the center or mass or, equivalently, on the local velocity. This trend should then be reflected in a clear correlation between isospin content and kinetic energy of the formed *IMF*'s, ³⁴.

5. Isospin Transport in Peripheral Collisions at the Fermi Energies

Now we investigate peripheral collisions between similar systems with different isospin, specifically collisions of different combinations of *Sn* isotopes. The isospin is used here both as a tracer of the reaction mechanism, as well as an observable of interest with respect to the iso-EOS. In the previous sections we have seen the isospin dynamics in instability regions and fragment formation. Here we study more directly the isospin transport in binary events. A neck of density below normal density develops between the two heavy residues, the evolution of which is driven by the motion of the spectators. During this phase isospin is transferred to the neck due to the density difference between the neck and the residues; this effect is called isospin migration, which leads to a more neutron-rich neck. In addition in collision systems with different asymmetry isospin is transported through neck due to the asymmetry gradient leading to an equilibration of the isospin of the residues, which has been called isospin diffusion. Thus in asymmetric systems there is a competition of isospin migration and diffusion.

The isospin transport can be discussed in a compact way by means of the chemical potentials for protons and neutrons as a function of density ρ and isospin I ³⁵. From this the p/n currents can be expressed as

$$\mathbf{j}_{p/n} = D_{p/n}^{\rho} \nabla \rho - D_{p/n}^I \nabla I \quad (4)$$

with $D_{p/n}^{\rho}$ the drift, and $D_{p/n}^I$ the diffusion coefficients for transport, which are

given explicitly in ref. ³⁵. Of interest here are the differences of currents between protons and neutrons which have a simple relation to the density dependence of the symmetry energy

$$\begin{aligned} D_n^\rho - D_p^\rho &\propto 4I \frac{\partial E_{sym}}{\partial \rho}, \\ D_n^I - D_p^I &\propto 4\rho E_{sym}. \end{aligned} \quad (5)$$

Thus the isospin transport due to density gradients, i.e. isospin migration, depends on the slope of the symmetry energy, or the symmetry pressure, while the transport due to isospin concentration gradients, i.e. isospin diffusion, depends on the absolute value of the symmetry energy. In peripheral collisions discussed here, residues of about normal density are in contact with the neck region of density below saturation density. In this region of density a stiff iso-EOS has a smaller value but a larger slope compared to a soft iso-EOS. Correspondingly we expect opposite effects of these models on the migration and diffusion of isospin.

We will in particular discuss the so-called Imbalance Ratio (also called Rami- or transport-ratio), which is defined as ³⁶

$$R_{P,T}^x = \frac{2x^M - (x^H + x^L)}{(x^H - x^L)}. \quad (6)$$

Here, x is an isospin sensitive quantity that is to be investigated with respect to equilibration, as e.g. the asymmetry $I = (N - Z)/(N + Z)$ which is considered here primarily, but also other quantities, such as isoscaling coefficients, ratios of production of light fragments, etc. The indices H and L refer to the symmetric reaction between the heavy (n-rich) and the light (n-poor) systems, while M refers to the mixed reaction. P, T denote the rapidity region, in which this quantity is measured, in particular the projectile and target rapidity regions. Clearly, this ratio is ± 1 in the projectile and target region, respectively, for complete transparency, and oppositely for complete rebound, while it is zero for complete equilibration.

Correlation with kinetic energy loss

The centrality dependence of the Imbalance Ratio, for (Sn,Sn) collisions, has been investigated in experiments ³⁷ as well as in theory ^{35,38} with rather promising results for the sensitivity to the symmetry term stiffness. We propose here a new analysis which appears experimentally more selective. The interaction time certainly influences the amount of isospin equilibration, see refs. ^{35,39}. On the other hand, longer interaction times should be correlated to a larger dissipation. The dissipation, in turn, has been measured, i.e. in deep inelastic collisions, by the kinetic energy loss.

In Fig.3 we present the imbalance ratio as a function of the relative energy loss (H:124Sn, L:112Sn, two beam energies 35 and 50A MeV). In the upper panel we separate the results for Momentum Dependent and Independent (MD vs MI)

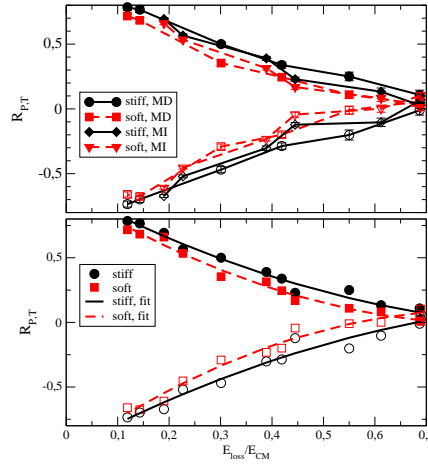


Fig. 3. Imbalance ratio as a function of relative energy loss: (upper panel) Separately for stiff (solid) and soft (dashed) iso-EOS, and for MD (circles and diamonds) and MI (squares and triangles) interactions, in the projectile region (full symbols) and the target region (open symbols). (lower panel) Quadratic fit to all points for the stiff (solid), resp. soft (dashed) iso-EOS.

interactions and stiff and soft iso-EOS, in each case the results for 35 and 50 MeV are collected together and connected by lines. We now see that the points for the different incident energies approximately fall on one line, however with some scatter around it.

The curves for the soft EOS (dashed) are generally lower in the projectile region (and oppositely for the target region), i.e. show more equilibration, than those for the stiff EOS. In order to emphasize this trend we have, in the lower panel of the figure, collected together the values for the stiff (circles, solid) and the soft (squares, dashed) iso-EOS, and fitted them by a quadratic curve. It is seen that this fit gives a good representation of the trend of the results.

The difference between the curves for the stiff and soft iso-EOS in the lower panel then isolates the effect of the iso-EOS from kinematical effects depending on the interaction time. It is seen, that there is a systematic effect of the symmetry energy of the order of about 20 percent, which should be measurable. The correlation suggested in Fig.3 should represent a general feature of isospin diffusion, and it would be of great interest to verify it experimentally.

6. Relativistic Collisions

Finally we focus our attention on relativistic heavy ion collisions, that provide a unique terrestrial opportunity to probe the in-medium nuclear interaction at high densities. An effective Lagrangian approach to the hadron interacting system is extended to the isospin degree of freedom: within the same frame equilibrium

properties (*EoS*, ⁴⁰) and transport dynamics ^{41,42} can be consistently derived. Within a covariant picture of the nuclear mean field, for the description of the symmetry energy at saturation (a) only the Lorentz vector ρ mesonic field, and (b) both, the vector ρ (repulsive) and scalar δ (attractive) effective fields ^{43,44} can be included. In the latter case the competition between scalar and vector fields leads to a stiffer symmetry term at high density ^{43,1}. The presence of the hadronic medium leads to effective masses and momenta $M^* = M + \Sigma_s$, $k^{*\mu} = k^\mu - \Sigma^\mu$, with Σ_s , Σ^μ scalar and vector self-energies. For asymmetric matter the self-energies are different for protons and neutrons, depending on the isovector meson contributions. We will call the corresponding models as *NLρ* and *NLρδ*, respectively, and just *NL* the case without isovector interactions.

For the more general *NLρδ* case the self-energies of protons and neutrons read:

$$\Sigma_s(p, n) = -f_\sigma \sigma(\rho_s) \pm f_\delta \rho_{s3}, \quad \Sigma^\mu(p, n) = f_\omega j^\mu \mp f_\rho j_3^\mu, \quad (n : \text{upper signs}), \quad (7)$$

where $\rho_s = \rho_{sp} + \rho_{sn}$, $j^\alpha = j_p^\alpha + j_n^\alpha$, $\rho_{s3} = \rho_{sp} - \rho_{sn}$, $j_3^\alpha = j_p^\alpha - j_n^\alpha$ are the total and isospin scalar densities and currents and $f_{\sigma, \omega, \rho, \delta}$ are the coupling constants of the various mesonic fields. $\sigma(\rho_s)$ is the solution of the non linear equation for the σ field ^{43,1}. For the description of heavy ion collisions we solve the covariant transport equation of the Boltzmann type ^{41,42} within the Relativistic Landau Vlasov (*RLV*) method, using phase-space Gaussian test particles ⁴⁵, and applying a Monte-Carlo procedure for the hard hadron collisions. The collision term includes elastic and inelastic processes involving the production/absorption of the $\Delta(1232 \text{ MeV})$ and $N^*(1440 \text{ MeV})$ resonances as well as their decays into pion channels, ^{46,47}. A larger repulsive vector contribution to the neutron energies is given by the ρ -coupling. This is rapidly increasing with density when the δ field is included ^{43,1}. As a consequence we expect a good sensitivity to the covariant structure of the isovector fields in nucleon emission and particle production data. Moreover the presence of a *Lorentz magnetic* term in the relativistic transport equation ^{41,42,1} will enhance the dynamical effects of vector fields ⁴⁸.

Isospin Flows

(n,p) flow differences will be directly affected. In ref. ⁴⁸ transverse and elliptic flows results are shown for the $^{132}\text{Sn} + ^{124}\text{Sn}$ reaction at 1.5 AGeV ($b = 6 \text{ fm}$). The effect of the different structure of the isovector channel is clear. Particularly evident is the splitting in the high p_t region of the elliptic flow. In the $(\rho + \delta)$ dynamics the high- p_t neutrons show a much larger *squeeze-out*. This is fully consistent with an early emission (more spectator shadowing) due to the larger ρ -field in the compression stage.

Isospin effects on sub-threshold kaon production at intermediate energies

Kaon production has been proven to be a reliable observable for the high density *EoS* in the isoscalar sector ^{50,51} Here we show that the $K^{0,+}$ production (in par-

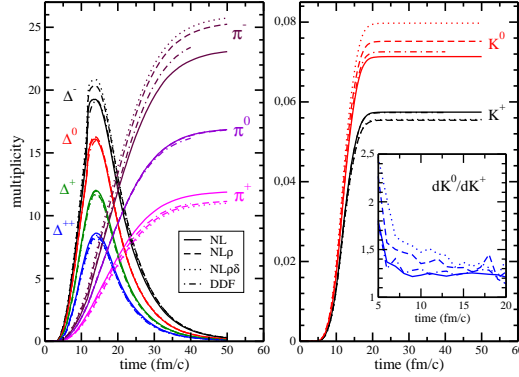


Fig. 4. Time evolution of the $\Delta^{\pm,0,++}$ resonances and pions $\pi^{\pm,0}$ (left), and kaons ($K^{+,0}$ (right) for a central ($b = 0$ fm impact parameter) Au+Au collision at 1 AGeV incident energy. Transport calculation using the NL , $NL\rho$, $NL\rho\delta$ and DDF models for the isovector part of the nuclear EoS are shown. The inset contains the differential K^0/K^+ ratio as a function of the kaon emission time.

ticular the K^0/K^+ yield ratio) can be also used to probe the isovector part of the EoS , 47,52.

Using our *RMF* transport approach we have analyzed pion and kaon production in central $^{197}\text{Au} + ^{197}\text{Au}$ collisions in the $0.8 - 1.8$ AGeV beam energy range, comparing models giving the same “soft” EoS for symmetric matter and with different effective field choices for E_{sym} . We will use three Lagrangians with constant nucleon-meson couplings ($NL...$ type, see before) and one with density dependent couplings (DDF , see 44), recently suggested for better nucleonic properties of neutron stars 53,54.

Fig. 4 reports the temporal evolution of $\Delta^{\pm,0,++}$ resonances, pions ($\pi^{\pm,0}$) and kaons ($K^{+,0}$) for central Au+Au collisions at 1 AGeV. It is clear that, while the pion yield freezes out at times of the order of $50\text{fm}/c$, i.e. at the final stage of the reaction (and at low densities), kaon production occur within the very early (compression) stage, and the yield saturates at around $20\text{fm}/c$. Consistently, as shown in the insert, larger isospin effects are expected for emitted kaons.

When isovector fields are included the symmetry potential energy in neutron-rich matter is repulsive for neutrons and attractive for protons. In a *HIC* this leads to a fast, pre-equilibrium, emission of neutrons. Such a *mean field* mechanism, often referred to as isospin fractionation 49,1, is responsible for a reduction of the neutron to proton ratio during the high density phase, with direct consequences on particle production in inelastic NN collisions.

Threshold effects represent a more subtle point. The energy conservation in a hadron collision in general has to be formulated in terms of the canonical momenta, i.e. for a reaction $1+2 \rightarrow 3+4$ as $s_{in} = (k_1^\mu + k_2^\mu)^2 = (k_3^\mu + k_4^\mu)^2 = s_{out}$. Since hadrons are propagating with effective (kinetic) momenta and masses, an equivalent relation should be formulated starting from the effective in-medium quantities $k^{*\mu} = k^\mu - \Sigma^\mu$

and $m^* = m + \Sigma_s$, where Σ_s and Σ^μ are the scalar and vector self-energies, Eqs.(7). The self-energy contributions will influence the particle production at the level of thresholds as well as of the phase space available in the final channel.

In the few AGeV region the effect is larger for the K^0/K^+ compared to the π^-/π^+ ratio. This is due to the subthreshold production and to the fact that the isospin effect enters twice in the two-step production of kaons, see ⁴⁷. Interestingly the Iso-*EoS* effect for pions is increasing at lower energies, when approaching the production threshold.

We have to note that in a study of kaon production in excited nuclear matter the dependence of the K^0/K^+ yield ratio on the effective isovector interaction appears much larger (see Fig.8 of ref.⁴⁶). The point is that in the non-equilibrium case of a heavy ion collision the asymmetry of the source where kaons are produced is in fact reduced by the $n \rightarrow p$ “transformation”, due to the favored $nn \rightarrow p\Delta^-$ processes. This effect is almost absent at equilibrium due to the inverse transitions, see Fig.3 of ref.⁴⁶. Moreover in infinite nuclear matter even the fast neutron emission is not present. This result clearly shows that chemical equilibrium models can lead to uncorrect results when used for transient states of an *open* system.

7. Testing Deconfinement at High Isospin Density

The hadronic matter is expected to undergo a phase transition into a deconfined phase of quarks and gluons at large densities and/or high temperatures. On very general grounds, the transition’s critical densities are expected to depend on the isospin of the system, but no experimental tests of this dependence have been performed so far.

Here we suggest the possibility of an *earlier* transition density to a mixed phase in isospin asymmetric systems ⁵⁵. Concerning the hadronic phase, we use the relativistic non-linear model of Glendenning-Moszkowski (in particular the “soft” *GM3* choice) ⁵⁶, where the isovector part is treated just with ρ meson coupling, and the iso-stiffer *NL* $\rho\delta$ interaction. For the quark phase we consider the *MIT* bag model with various bag pressure constants. In particular we are interested in those parameter sets which would allow the existence of quark stars ⁵⁷, i.e. parameters sets for which the so-called Witten-Bodmer hypothesis is satisfied ^{58,59}. One of the aim of our work it to show that if quark stars are indeed possible, it is then very likely to find signals of the formation of a mixed quark-hadron phase in intermediate-energy heavy-ion experiments ⁵⁵.

The structure of the mixed phase is obtained by imposing the Gibbs conditions ^{60,61} for chemical potentials and pressure and by requiring the conservation of the total baryon and isospin densities

$$\begin{aligned}\mu_B^{(H)} &= \mu_B^{(Q)}, \quad \mu_3^{(H)} = \mu_3^{(Q)}, \\ P^{(H)}(T, \mu_{B,3}^{(H)}) &= P^{(Q)}(T, \mu_{B,3}^{(Q)}), \\ \rho_B &= (1 - \chi)\rho_B^H + \chi\rho_B^Q,\end{aligned}$$

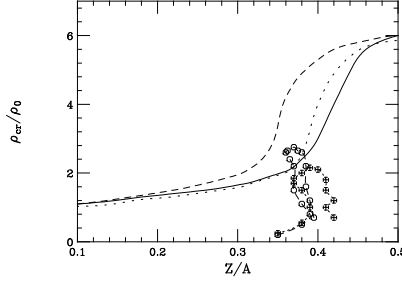


Fig. 5. Variation of the transition density with proton fraction for various hadronic *EoS* parameterizations. Dotted line: *GM3* parameterization; dashed line: *NLρ* parameterization; solid line: *NLρδ* parameterization. For the quark *EoS*, the *MIT* bag model with $B^{1/4}=150$ MeV. The points represent the path followed in the interaction zone during a semi-central $^{132}\text{Sn}+^{132}\text{Sn}$ collision at 1 AGeV (circles) and at 300 AMeV (crosses).

$$\rho_3 = (1 - \chi)\rho_3^H + \chi\rho_3^Q, \quad (8)$$

where χ is the fraction of quark matter in the mixed phase. In this way we get the *binodal* surface which gives the phase coexistence region in the (T, ρ_B, ρ_3) space. For a fixed value of the conserved charge ρ_3 we will study the boundaries of the mixed phase region in the (T, ρ_B) plane. In the hadronic phase the charge chemical potential is given by $\mu_3 = 2E_{\text{sym}}(\rho_B) \frac{\rho_3}{\rho_B}$. Thus, we expect critical densities rather sensitive to the isovector channel in the hadronic *EoS*.

In Fig. 5 we show the crossing density ρ_{cr} separating nuclear matter from the quark-nucleon mixed phase, as a function of the proton fraction Z/A . We can see the effect of the δ -coupling towards an *earlier* crossing due to the larger symmetry repulsion at high baryon densities. In the same figure we report the paths in the $(\rho, Z/A)$ plane followed in the c.m. region during the collision of the n-rich $^{132}\text{Sn}+^{132}\text{Sn}$ system, at different energies. At 300 AMeV we are just reaching the border of the mixed phase, and we are well inside it at 1 AGeV. We expect a *neutron trapping* effect, supported by statistical fluctuations as well as by a symmetry energy difference in the two phases. In fact while in the hadron phase we have a large neutron potential repulsion (in particular in the *NLρδ* case), in the quark phase we only have the much smaller kinetic contribution. Observables related to such neutron “trapping” could be an inversion in the trend of the formation of neutron rich fragments and/or of the π^-/π^+ , K^0/K^+ yield ratios for reaction products coming from high density regions, i.e. with large transverse momenta. In general we would expect a modification of the rapidity distribution of the emitted “isospin”, with an enhancement at mid-rapidity joint to large event by event fluctuations..

8. Perspectives

We have shown that *violent* collisions of n-rich heavy ions from low to relativistic energies can bring new information on the isovector part of the in-medium interaction, qualitatively different from equilibrium *EoS* properties. We have presented

quantitative results in a wide range of beam energies. At low energies we see isospin effects on the dissipation in deep inelastic collisions, at Fermi energies the Iso-EoS sensitivity of the isospin transport in fragment reactions and finally at intermediate the dependence of differential flows on the $Iso - MD$ and effective mass splitting. In relativistic collisions we have shown the possibility of a direct *measure* of the Lorentz structure of the isovector fields at high baryon density. We have presented quantitative results for differential collective flows and yields of charged pion and kaon ratios. Important non-equilibrium effects for particle production are stressed. Finally our study supports the possibility of observing precursor signals of the phase transition to a mixed hadron-quark matter at high baryon density in the collision, central or semi-central, of neutron-rich heavy ions in the energy range of a few GeV per nucleon. In conclusion the results presented in this "Isospin Journey" appear very promising for the possibility of exciting new results from dissipative collisions with radioactive beams.

Acknowledgements. We warmly thanks A.Drago and A.Lavagno for the intense collaboration on the mixed hadron-quark phase transition at high baryon and isospin density.

References

1. V.Baran, M.Colonna, V.Greco, M.Di Toro, *Phys. Rep.* **410** (2005) 335.
2. C.Fuchs, H.H.Wolter, *Eur. Phys. Jour.* **A30** (2006) 5.
3. A.Guarnera, M.Colonna, P.Chomaz, *Phys. Lett.* **B373** (1996) 267.
4. M.Colonna et al., *Nucl. Phys.* **A642** (1998) 449.
5. P.Chomaz, M.Colonna, J.Randrup, *Phys. Rep.* **389** (2004) 263.
6. M.Colonna, M. Di Toro, G. Fabbri, S. Maccarone, *Phys. Rev.* **C57** (1998) 1410.
7. P. Chomaz, M. Di Toro, A.Smerzi, *Nucl. Phys.* **A563** (1993) 509.
8. P. F. Bortignon et al., *Nucl. Phys.* **A583** (1995) 101c.
9. S. Flibotte et al., *Phys. Rev. Lett.* **77** (1996) 1448.
10. M. Cinausero et al., *Nuovo Cimento* **111** (1998) 613.
11. D. Pierrousakou et al., *Eur. Phys. Jour.* **A16** (2003) 423, *Nucl. Phys.* **A687** (2003) 245c.
12. F.Amorini et al., *Phys. Rev.* **C69** (2004) 014608.
13. D. Pierrousakou et al., *Phys. Rev.* **C71** (2005) 054605.
14. B.Martin, D. Pierrousakou et al. (Medea Collab.), *Prompt Dipole Radiation in Fusion Reactions*, arXiv:0710.1512[nucl-ex], *Phys. Rev. Lett.* submitted.
15. D. M. Brink and M. Di Toro, *Nucl. Phys.* **A372** (1981) 151.
16. V. Baran et al., *Nucl. Phys.* **A600** (1996) 111.
17. V. Baran et al., *Nucl. Phys.* **A679** (2001) 373.
18. C. Simenel et al., *Phys. Rev. Lett.* **86** (2000) 2971.
19. V. Baran, D. M. Brink, M. Colonna, M. Di Toro, *Phys. Rev. Lett.* **87** (2001) 182501
20. L. Bonanno, *Effetti di radiazione diretta dipolare sulla sintesi degli elementi superpesanti*, Master Thesis, Catania Univ. 2004.
21. M.Lewitowicz, *Challenges of the SPIRAL 2 Project*, NN06 Conf., Rio de Janeiro; <http://ganinfo.in2p3.fr/research/developments/spiral2>
22. Letter of Intent for the new SPIRAL2 Facility at GANIL.
23. M.Colonna, M.Di Toro, A.Guarnera, *Nucl. Phys.* **A589** (1995) 160.

24. M.Di Toro, A.Olmi, R.Roy, *Eur. Phys. Jour.* **A30** (2006) 65.
25. V.Baran et al., *Phys. Rev.* **C72** (2005) 064620.
26. V.Baran, M.Colonna, M.Di Toro, *Nucl. Phys.* **A730** (2004) 329.
27. E.De Filippo et al. (Chimera Collab.), *Phys. Rev.* **C71** (2005) 044602; *Phys. Rev.* **C71** (2005) 064604.
28. R.Lionti, V.Baran, M.Colonna, M.Di Toro, *Phys. Lett.* **B625** (2005) 33.
29. J.Wilczynski et al. (Chimera Collab.), *Int. Jour. Mod. Phys.* **E14** (2005) 353.
30. E. De Filippo et al. (Chimera Collab.), *Time scales and isospin effects on reaction dynamics*, contribution to the NN06 Conf., Rio de Janeiro, August 2006.
31. H.Mueller and B.D.Serot, *Phys.Rev.* **C52** (1995) 2072.
32. Bao-An Li and C.M.Ko, *Nucl.Phys.* **A618** (1997) 498.
33. V. Baran et al., *Nucl.Phys.* **A703** (2002) 603.
34. M.Colonna et al., arXiv:0707.3092 [nucl-th], *Phys.Rev.Lett.* submitted
35. V.Baran et al., *Phys.Rev.* **C72** (2005) 064620.
36. F.Rami et al., *Phys.Rev.Lett.* **84** (2000) 1120.
37. M.B. Tsang, et al., *Phys. Rev. Lett.* **92**, 062701 (2004)
38. B.A. Li, L.W. Chen, *Phys. Rev. C* **72**, 064611 (2005);
L.W. Chen, C.M. Ko, B.A. Li, *Phys. Rev. Lett* **94**, 032701 (2005)
39. J.Rizzo et al., *Investigation of the Isovector EOS in Peripheral Heavy Ion Collisions at Fermi Energies*, *Nucl.Phys.* **A** submitted.
40. B. D. Serot, J. D. Walecka, *Advances in Nuclear Physics*, **16**, 1, eds. J. W. Negele, E. Vogt, (Plenum, N.Y., 1986).
41. C. M. Ko, Q. Li, R. Wang, *Phys. Rev. Lett.* **59** (1987) 1084.
42. B. Blättel, V. Koch, U. Mosel, *Rep. Prog. Phys.* **56** (1993) 1.
43. B. Liu, V. Greco, V. Baran, M. Colonna, M. Di Toro, *Phys. Rev.* **C65** (2002) 045201.
44. T. Gaitanos, et al., *Nucl. Phys.* **A732** (2004) 24.
45. C. Fuchs. H.H. Wolter, *Nucl. Phys.* **A589** (1995) 732.
46. G. Ferini, M. Colonna, T. Gaitanos, M. Di Toro, *Nucl. Phys.* **A762** (2005) 147.
47. G.Ferini et al., *Phys. Rev. Lett.* **97** (2006) 202301.
48. V. Greco et al., *Phys. Lett.* **B562** (2003) 215.
49. B.A. Li, W.U. Schroeder (Eds.), *Isospin Physics in Heavy-Ion Collisions at Intermediate Energies*, Nova Science, New York, 2001.
50. C. Fuchs, *Prog.Part.Nucl.Phys.* **56** 1-103 (2006).
51. C.Hartnack, H.Oeschler, J.Aichelin, *Phys. Rev. Lett.* **96** (2006) 012302.
52. V.Prassa et al., *Nucl.Phys.* **A789** (2007) 311.
53. T.Klähn et al., *Phys. Rev.* **C74** (2006) 035802.
54. B.Liu et al., *Phys. Rev.* **C75** (2007) 048801.
55. M. Di Toro, A. Drago, T. Gaitanos, V. Greco, A. Lavagno, *Nucl. Phys.* **A775** (2006) 102.
56. N.K.Glendenning, S.A.Moszkowski, *Phys. Rev. Lett.* **67** (1991) 2414.
57. A.Drago, A.Lavagno, *Phys. Lett.* **B511** (2001) 229.
58. E.Witten, *Phys. Rev.* **D30** (1984) 272.
59. A.R.Bodmer, *Phys. Rev.* **D4** (1971) 1601.
60. L.D.Landau, L.Lifshitz, *Statistical Physics*, Pergamon Press, Oxford 1969.
61. N.K.Glendenning, *Phys. Rev.* **D46** (1992) 1274.